

Magnetic and magnetocaloric properties of Cu-substituted $\text{La}_{1-x}\text{Pb}_x\text{MnO}_3$ ($x = 0.14$) single crystals

B. C. Zhao, Y. P. Sun, X. B. Zhu, and W. H. Song

Citation: *J. Appl. Phys.* **101**, 053920 (2007); doi: 10.1063/1.2561344

View online: <http://dx.doi.org/10.1063/1.2561344>

View Table of Contents: <http://jap.aip.org/resource/1/JAPIAU/v101/i5>

Published by the [American Institute of Physics](#).

Related Articles

History dependence of directly observed magnetocaloric effects in (Mn, Fe)As
Appl. Phys. Lett. **100**, 252409 (2012)

The magnetocaloric effect of partially crystalline Fe-B-Cr-Gd alloys
J. Appl. Phys. **111**, 113919 (2012)

Normal or inverse magnetocaloric effects at the transition between antiferromagnetism and ferromagnetism
Appl. Phys. Lett. **100**, 242408 (2012)

On the Curie temperature dependency of the magnetocaloric effect
Appl. Phys. Lett. **100**, 242407 (2012)

Spin reorientation and the magnetocaloric effect in $\text{Ho}_y\text{Er}_{1-y}\text{N}$
J. Appl. Phys. **111**, 113916 (2012)

Additional information on *J. Appl. Phys.*

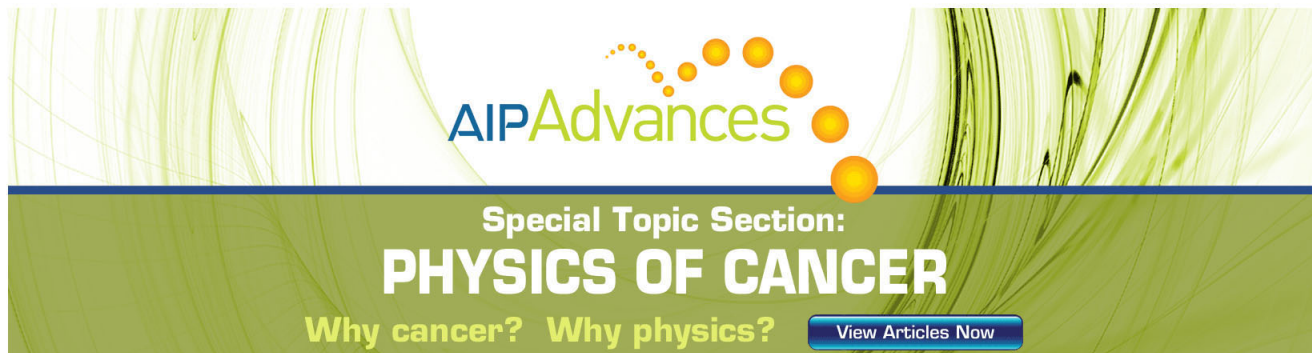
Journal Homepage: <http://jap.aip.org/>

Journal Information: http://jap.aip.org/about/about_the_journal

Top downloads: http://jap.aip.org/features/most_downloaded

Information for Authors: <http://jap.aip.org/authors>

ADVERTISEMENT



Special Topic Section:
PHYSICS OF CANCER

Why cancer? Why physics? [View Articles Now](#)

Magnetic and magnetocaloric properties of Cu-substituted $\text{La}_{1-x}\text{Pb}_x\text{MnO}_3$ ($x \sim 0.14$) single crystals

B. C. Zhao, Y. P. Sun,^{a)} X. B. Zhu, and W. H. Song

Key Laboratory of Materials Physics, Institute of Solid State Physics,
and Hefei High Magnetic Field Laboratory, Chinese Academy of Sciences, Hefei 230031, China

(Received 15 September 2006; accepted 31 December 2006; published online 15 March 2007)

Structural, magnetic, and magnetocaloric properties in perovskite manganites $\text{La}_{1-x}\text{Pb}_x\text{Mn}_{1-y-z}\text{Cu}_y\text{O}_3$ ($x \sim 0.14$, $y=0, 0.01, 0.02$, $z=0.02, 0.08, 0.11$) single crystals have been investigated. The Curie temperature T_C decreases monotonously with increasing Cu-doping concentration. A sharp downturn in the inverse magnetic susceptibility $1/\chi_m$ vs T plot at Griffiths temperature T_G well above T_C was observed for the free-doped sample, which can be attributed to the appearance of spin cluster in the paramagnetic state. The temperature interval between T_G and T_C decreases with increasing Cu-doping level and almost disappears as Cu concentration reaches 0.02. Large magnetic entropy change ΔS_M occurs near T_C and ΔS_M approaches a maximum value for the sample with Cu-doping level $y=0.01$. The result can be explained based on the competing effect between the double-exchange interaction and the lattice distortion induced by Cu doping.

© 2007 American Institute of Physics. [DOI: 10.1063/1.2561344]

I. INTRODUCTION

Magnetocaloric effect (MCE) in various magnetic materials has attracted considerable attention due to its potential applications on environmental concerns and energy saving.¹⁻⁵ MCE is known as an isothermal magnetic entropy change (ΔS_M) or an adiabatic temperature change of a material upon the application or removal of a magnetic field. In general, MCE is proportional to the magnitude of the magnetic moment and the applied magnetic field. The rare-earth element gadolinium and its compounds with high magnetization are therefore considered to be possible materials exhibiting a large MCE near room temperature. However, the application of gadolinium is limited due to its high cost.

Recently, perovskite manganites have been extensively studied because their MCE, Curie temperature, and saturated magnetization strongly depends on dopants. These materials are believed to be good candidates for magnetic refrigeration at various temperature ranges.⁶⁻⁸ Unfortunately, the nonuniform distribution of the magnetic entropy change ΔS_M , which is detrimental to the magnetic refrigerator, was found in the polycrystalline perovskite manganites due to the structural inhomogeneity. On the contrary, the study of MCE in manganite single crystals is of great interest, because the absence of grain boundaries in these materials would be expected to show a uniform ΔS_M distribution, which is desirable for an Ericson-cycle magnetic refrigerator. In this work, we report on our study of structural, magnetic, and magnetocaloric properties of the Cu-substituted perovskite manganites $\text{La}_{1-x}\text{Pb}_x\text{MnO}_3$ ($x \sim 0.14$) single crystals.

II. EXPERIMENT

Single crystals of $\text{La}_{1-x}\text{Pb}_x\text{Mn}_{1-y-z}\text{Cu}_y\text{O}_3$ ($x=0.14$, $y=0, 0.01, 0.02$, $z=0.02, 0.08, 0.11$) were grown by flux

melt technique using the PbO-PbF_2 (1:1) flux.⁹ In the following text, the three studied samples are denoted as $y=0, 0.01$, and 0.02 , respectively. Growth precursors La_2O_3 , PbO , MnO_2 , CuO , and PbF_2 were weighed in an appropriate ratio and homogenized in an agate pestle. The homogenized mixture was transferred into a platinum crucible and the growth was carried out in a resistive furnace. The furnace was first heated to 1250°C and held at this temperature for 20 h to ensure the sufficient dissolution of the raw materials, then cooled to 980°C at a rate of 1.5°C/h . After these steps the furnace was cooled rapidly to room temperature to avoid possible twinning. Black cubic-like single crystals of several millimeters in dimension were separated mechanically for investigation. Crystal structure and phase purity were examined by powder and single-crystal x-ray diffraction (XRD) using $\text{Cu } K\alpha$ radiation at room temperature. The composition of the studied crystals is determined by inductively coupled plasma and Auger electron spectroscopy (ICP-AES) techniques. Magnetic measurements were performed with a Quantum Design superconducting quantum interference device (SQUID) magnetometer ($2 \leq T \leq 400$ K, $0 \leq H \leq 5$ T).

III. RESULTS AND DISCUSSION

Black cubic-like single crystals were extracted from the exposed surface and cavities within the solidified flux. The average size of the single crystal increases initially and then decreases with increasing Cu-doping concentration. This indicates that the light Cu doping may be useful to the growth of the single crystals. The actual stoichiometry of the obtained single crystals ascertained by ICP-AES technique and the nominal composition of the initial mixture are shown in Table I. It shows that the Pb concentration in all samples does not exceed 0.15, although the initial nominal Pb concentration is fixed at 0.3, implying that there exists a threshold of the Pb solubility in these flux growth Cu-doped $\text{La}_{1-x}\text{Pb}_x\text{MnO}_3$ single crystals. The Cu content increases with

^{a)}Corresponding author; electronic mail: ypsun@issp.ac.cn

TABLE I. Nominal compositions and actual compositions determined by ICP analysis of the $\text{La}_{1-x}\text{Pb}_x\text{Mn}_{1-y-z}\text{Cu}_y\text{O}_3$ ($x \sim 0.14$) single crystals.

Nominal composition	Actual compositions
$\text{La}_{0.7}\text{Pb}_{0.3}\text{MnO}_3$	$\text{La}_{0.87}\text{Pb}_{0.13}\text{Mn}_{0.98}\text{O}_\delta$
$\text{La}_{0.7}\text{Pb}_{0.3}\text{Mn}_{0.9}\text{Cu}_{0.1}\text{O}_3$	$\text{La}_{0.86}\text{Pb}_{0.14}\text{Mn}_{0.91}\text{Cu}_{0.01}\text{O}_\delta$
$\text{La}_{0.7}\text{Pb}_{0.3}\text{Mn}_{0.8}\text{Cu}_{0.2}\text{O}_3$	$\text{La}_{0.85}\text{Pb}_{0.15}\text{Mn}_{0.87}\text{Cu}_{0.02}\text{O}_\delta$

increasing initial nominal Cu concentration, but the actual Cu content in the grown single crystal is much smaller than the initial nominal Cu-doping level.

Figure 1(a) shows the powder XRD patterns of $\text{La}_{1-x}\text{Pb}_x\text{Mn}_{1-y-z}\text{Cu}_y\text{O}_3$ single crystals at room temperature. It shows that all samples are single phase with no detectable secondary phases. The Cu doping at Mn site does not change the crystal structure symmetry of the sample. All peaks of the XRD patterns can be indexed with a rhombohedral lattice with the space group $R\bar{3}c$ (No. 167) in the whole doping level range. The result is consistent with that of the polycrystalline $\text{La}_{0.7}\text{Pb}_{0.3}\text{MnO}_3$ reported previously.¹⁰ X-ray diffraction was also performed on the single crystals with x-ray illumination on their neighboring face (named *ab*, *bc*, and *ac*). A typical result for the sample with $y = 0.01$ is shown in Fig. 1(b), in which only sharp (001), (002), and (003) peaks are observed, implying the high quality of the crystal.

The temperature dependence of dc magnetization M for $\text{La}_{1-x}\text{Pb}_x\text{Mn}_{1-y-z}\text{Cu}_y\text{O}_3$ ($x \sim 0.14$, $y = 0, 0.1$, and 0.02) single crystals is shown in Fig. 2. The data were obtained in the heating process at zero-field-cooled (ZFC) mode under an applied magnetic field of $\mu_0 H = 0.01$ T in the temperature range of 5–390 K. It shows that all studied samples undergo a sharp paramagnetic-ferromagnetic (PM-FM) transition around Curie temperature T_C (defined as the one corresponding to the peak of dM/dT in the M vs T curve). The obtained T_C is 290, 287, and 267 K for the samples with $y = 0, 0.01$, and 0.02 , respectively. Both the magnitudes of M and T_C decrease monotonously with increasing Cu-doping concentration due to the diluted double-exchange (DE) effect in the

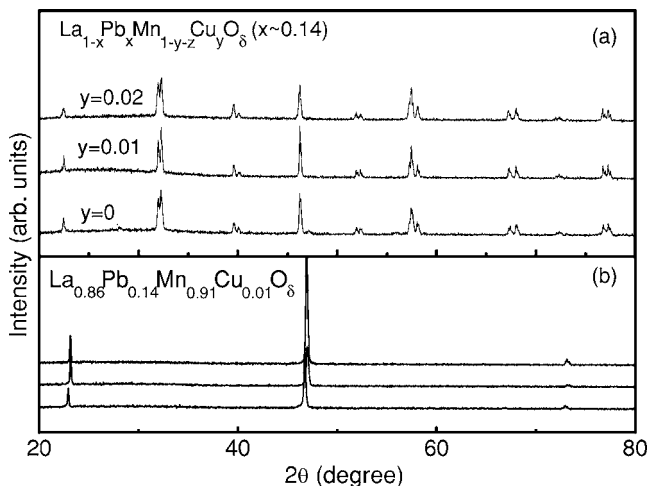


FIG. 1. (a) X-ray powder diffraction patterns for $\text{La}_{1-x}\text{Pb}_x\text{Mn}_{1-y-z}\text{Cu}_y\text{O}_3$ ($x \sim 0.14$) single crystals. (b) X-ray diffraction pattern of a $\text{La}_{0.86}\text{Pb}_{0.14}\text{Mn}_{0.91}\text{Cu}_{0.01}\text{O}_3$ single crystal.

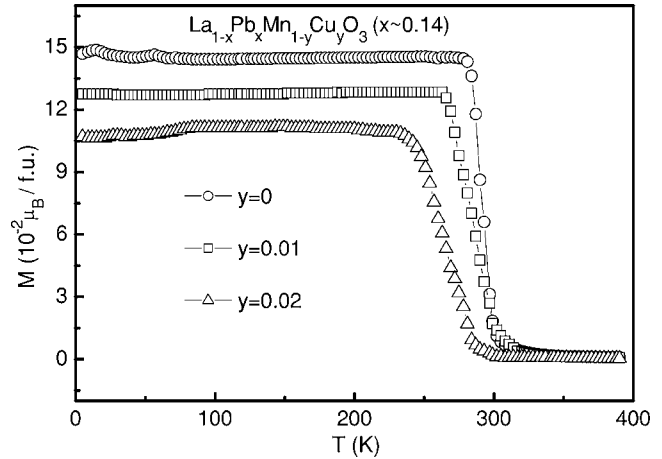


FIG. 2. Magnetization as a function of temperature for $\text{La}_{1-x}\text{Pb}_x\text{Mn}_{1-y-z}\text{Cu}_y\text{O}_3$ ($x \sim 0.14$, $y = 0, 0.1$, and 0.02) single crystals measured at $\mu_0 H = 0.01$ T under the zero-field-cooled (ZFC) mode.

crystals induced by Cu doping, which is similar to the Cu-doped polycrystalline samples.¹¹ The inverse magnetic susceptibility $1/\chi_m$ as a function of temperature for all studied samples is shown in Fig. 3. For the free-doped sample, Fig. 3 shows that there exists an obvious kink or downturn in the $1/\chi_m$ vs T plot at T_G (indicated by an arrow in Fig. 3) well above T_C . The temperature T_G can be considered as the Griffiths temperature,¹² which signified the appearance of $\text{Mn}^{3+}\text{-Mn}^{4+}$ spin clusters in the PM state before the long-range spin ordering is fully achieved at T_C . The existence of spin cluster in the PM state can be confirmed by the large effective magnetic moment deduced from the linear part of $1/\chi_m$ vs T plot, as described in Ref. 9. Moreover, the temperature interval between T_G and T_C is much smaller for the $y = 0.01$ sample (~ 30 K) compared to the free-doped sample (~ 50 K), and almost disappears as the Cu concentration reaches 0.02. In other words, the substitution of Cu for Mn in the crystal can destroy the spin cluster in the PM state. As discussed in Ref. 9, the occupation of Cu ions at Mn sites can bring local structural distortion and random Coulomb potential in the crystal, which can localize the charge carrier around Cu ions and result in the disappearance of the spin cluster in the PM phase.

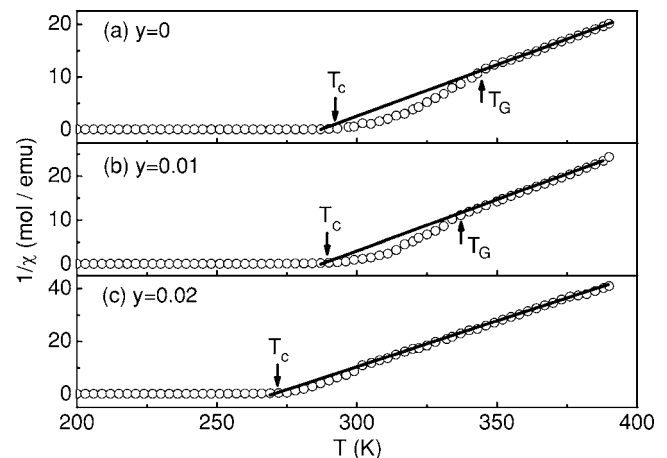


FIG. 3. Temperature dependence of inverse magnetic susceptibility $1/\chi_m$ for $\text{La}_{1-x}\text{Pb}_x\text{Mn}_{1-y-z}\text{Cu}_y\text{O}_3$ single crystals: (a) $y = 0$; (b) $y = 0.01$; (c) $y = 0.02$. The lines are calculated according to the Curie-Weiss law.

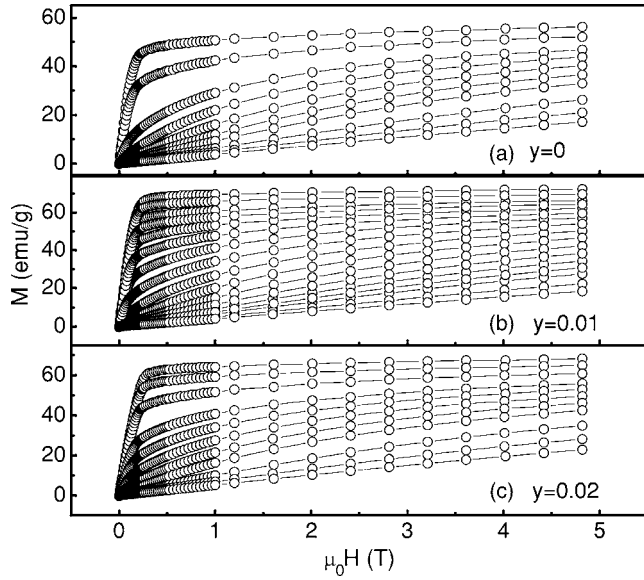


FIG. 4. Magnetic field dependence of the magnetization at various temperatures around T_C for $\text{La}_{1-x}\text{Pb}_x\text{Mn}_{1-y-z}\text{Cu}_y\text{O}_3$ ($x \sim 0.14$): (a) $y=0$; (b) $y=0.01$; (c) $y=0.02$.

Isothermal magnetization of all samples was measured at various temperatures in a narrow temperature interval around T_C , under magnetic fields up to 4.82 T. For each measurement, the sample was heated to a certain temperature well above T_C first, then, slowly cooled to the set temperature at zero magnetic fields. The results are presented in Fig. 4. It shows that there exists a drastic change of the magnetization around T_C , indicating a large ΔS_M may occur in these samples. According to the classical thermodynamical theory, ΔS_M induced by the variation of a magnetic field from 0 to H_{\max} is given by¹³

$$\Delta S_M(T, H) = S_M(T, H) - S_M(T, 0) = \int_0^{H_{\max}} \left(\frac{\partial M}{\partial T} \right)_H dH. \quad (1)$$

For the magnetization measured at small discrete magnetic field and temperature intervals, ΔS_M can be approximated as¹⁴

$$|\Delta S_M| = \sum_i \frac{M_i - M_{i+1}}{T_{i+1} - T_i} \Delta H_i, \quad (2)$$

where M_i and M_{i+1} are the experimental values of the magnetization at T_i and T_{i+1} , respectively. By measuring the isothermal M - H curve at various temperatures, one can calculate ΔS_M associated with the magnetic field variation from Eq. (2). In Fig. 5, ΔS_M is plotted against temperature for all samples at $\Delta H=1, 2, 3, 4$, and 4.82 T. As expected from Eq. (2), the peaks of ΔS_M for the three samples lie around their T_C where the variation of M with temperature is the sharpest and ΔS_M increases with increasing the variation of the applied magnetic field ΔH . The maximum magnetic entropy change corresponding to a magnetic field variation of 4.82 T is 5.0, 5.4, and 4.8 J/kg K for the samples with $y=0, 0.01$, and 0.02, respectively. It should be noted that the maximum of the magnetic entropy change for the studied crystals is

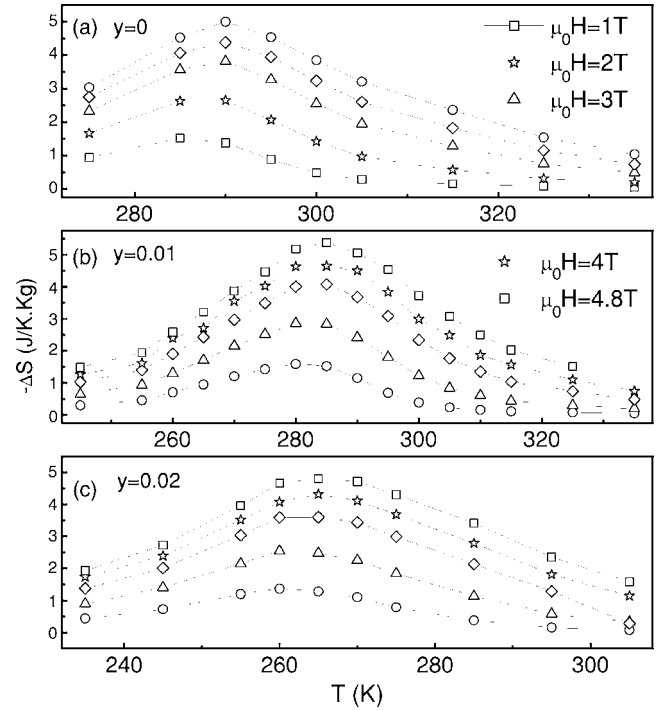


FIG. 5. Temperature dependence of the magnetic entropy change $-\Delta S_M$ in various applied magnetic fields for $\text{La}_{1-x}\text{Pb}_x\text{Mn}_{1-y-z}\text{Cu}_y\text{O}_3$ ($x \sim 0.14$): (a) $y=0$; (b) $y=0.01$; (c) $y=0.02$.

smaller than that of gadolinium or its compounds,¹⁵ however, the presently studied single crystal possesses some characteristics such as easier growing, higher chemical stability, and easier tuning of T_C by element doping. In addition, due to the absence of grain boundaries in the present manganite single crystals, the $\Delta S_M(T)$ distribution in these samples is much more uniform than that of gadolinium or polycrystalline manganites. All these results show that the present single crystals could be potential good working materials for magnetic refrigeration in household refrigerators or air conditioning. Another interesting feature of present samples is that the maximum of the magnetic entropy change occurs at the sample with $y=0.01$, although its T_C and saturated magnetization decrease monotonously with increasing Cu-doping content. For the sake of clarity, the Cu content y dependence of Curie temperature T_C , saturated magnetization M_S at 5 K, and maximum magnetic entropy change ΔS_M are plotted in Fig. 6. The result is inconsistent with that reported in other Mn-site substituted systems, where ΔS_M and T_C have the same change trend with impurity doping level.¹⁶ The origin of this phenomenon will be discussed below.

In general, the large ΔS_M in perovskite manganites mainly originates from the considerable variation of M near T_C . Moreover, the spin-lattice coupling in the magnetic ordering process also plays an important role in the large magnetic entropy change in manganites.⁸ In fact, significant lattice change accompanying magnetic transition in perovskite manganites due to strong coupling between spin and lattice has already been observed previously.¹⁷ The lattice change in Mn-O band distance and Mn-O-Mn band angle would in turn favor the spin ordering.¹⁸ Therefore, the abrupt reduction of M occurring near T_C results in a large ΔS_M . As discussed in

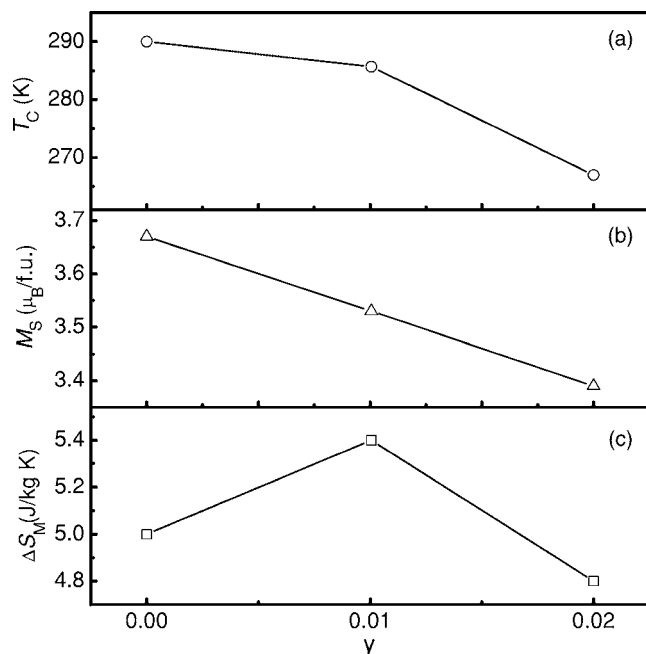


FIG. 6. (a) Cu concentration y dependence of Curie temperature T_C ; (b) saturated magnetization M_S at 5 K; and (c) maximum magnetic entropy change ΔS_M .

Ref. 9, the Cu substitution for Mn in present samples destroys the Mn-O-Mn bonds gradually and results in the weakening of DE interaction. As discussed above, the weakening of DE interaction may reduce ΔS_M of the crystal. At the same time, the unavoidable Mn-site deficiency due to Cu doping causes the local lattice distortion around Cu ions in the crystal. Therefore, it is suggested that the local lattice distortion could contribute additional entropy to the sample. That is to say, there are two competing components to determine the magnetic entropy in the present single crystals. As the Cu-doping concentration is small, the contribution of the local lattice distortion to the magnetic entropy plays a dominant role, so ΔS_M increases with Cu-doping concentration to $y=0.01$. With further increase of Cu, the contribution of the weakening of DE interaction to ΔS_M increases. Consequently, a smaller ΔS_M near T_C is observed for the sample with $y=0.02$.

IV. CONCLUSION

In summary, the structural, magnetic, and magnetocaloric properties of $\text{La}_{1-x}\text{Pb}_x\text{Mn}_{1-y-z}\text{Cu}_y\text{O}_3$ ($x \sim 0.14$, $y=0$,

0.01, and 0.02) single crystals were investigated. The Curie temperature T_C decreases monotonously with increasing Cu concentration. A sharp downturn in the $1/\chi_m$ vs T plot suggests that the existence of Griffiths phase in the samples with $y=0$ and 0.01. Griffiths phase can be destroyed due to Cu doping. Large magnetic entropy changes occur near T_C and the magnetic entropy change reaches a maximum value for the sample with $y=0.01$. The result can be explained based on the competing role of the DE interaction and the local lattice distortion induced by Cu doping.

ACKNOWLEDGMENTS

This work is supported by the National Key Basic Research under Contract No. 001CB610604, and the National Natural Science Foundation of China under Contract Nos. 10474100, 50672099, and Director's Fund of Hefei Institutes of Physical Science, Chinese Academy of Sciences.

- ¹V. K. Pecharsky and K. A. Gschneidner, Jr., *J. Magn. Magn. Mater.* **200**, 44 (1999).
- ²K. A. Gschneidner, Jr. and V. K. Pecharsky, *J. Appl. Phys.* **85**, 5365 (1999).
- ³X. Bohigas, J. Tejada, M. L. Marinez-Sarrion, and S. Tripp, *Appl. Phys. Lett.* **73**, 390 (1998).
- ⁴S. Yu. Dan'kov, *Phys. Rev. B* **57**, 3478 (1998).
- ⁵H. Wada and Y. Tanabe, *Appl. Phys. Lett.* **79**, 3302 (2001).
- ⁶M. H. Phan, S. C. Yu, and N. H. Hur, *Appl. Phys. Lett.* **86**, 072504 (2005).
- ⁷A. Szewczyk, H. Szymczak, A. Wisniewski, K. Piotrowski, R. Kartaszynski, B. Dabrowski, S. Kolesnik, and Z. Bukowski, *Appl. Phys. Lett.* **77**, 1026 (2000).
- ⁸Z. B. Guo, Y. W. Du, J. S. Zhu, H. Huang, W. P. Ding, and D. Feng, *Phys. Rev. Lett.* **78**, 1142 (1997).
- ⁹B. C. Zhao, W. H. Song, Y. Q. Ma, R. Ang, S. B. Zhang, and Y. P. Sun, *Phys. Rev. B* **72**, 132401 (2005).
- ¹⁰S. L. Young, H. Z. Chen, L. Horng, J. B. Shi, and Y. C. Chen, *Jpn. J. Appl. Phys., Part 1* **40**, 4878 (2001).
- ¹¹L. Pi, L. Zheng, and Y. H. Zhang, *Phys. Rev. B* **61**, 8917 (2000).
- ¹²R. B. Griffiths, *Phys. Rev. Lett.* **23**, 17 (1969).
- ¹³T. Hashimoto, T. Numasawa, M. Shino, and T. Okada, *Cryogenics* **21**, 647 (1981).
- ¹⁴M. Földeäki, R. Chahine, and T. K. Bose, *J. Appl. Phys.* **77**, 3528 (1995).
- ¹⁵V. K. Pecharsky and K. A. Gschneidner, *Appl. Phys. Lett.* **70**, 3299 (1997).
- ¹⁶X. Bohigas, E. del Barco, M. Sales, and J. Tejada, *J. Magn. Magn. Mater.* **196-197**, 455 (1999).
- ¹⁷P. G. Radaelli, D. E. Cox, M. Marezio, S.-W. Cheong, P. E. Schiffer, and A. P. Ramirez, *Phys. Rev. Lett.* **75**, 4488 (1995).
- ¹⁸M. H. Phan, H. X. Peng, S. C. Yu, and N. H. Hur, *J. Magn. Magn. Mater.* **290-291**, 665 (2005).